Degradation of the endoplasmic reticulum? anchored transcription factor MyRF by the ubiquitin ligase SCFFbxw7 in a manner dependent on the kinase GSK-3

中山，省悟

KYUSHU UNIVERSITY

Degradation of the endoplasmic reticulum–anchored transcription factor MyRF by the ubiquitin ligase SCF^{Fbxw7} in a manner dependent on the kinase GSK-3

Shogo Nakayama, Kanae Yumimoto, Atsuki Kawamura, and Keiichi I. Nakayama[1]

From the Department of Molecular and Cellular Biology, Medical Institute of Bioregulation, Kyushu University, 3-1-1 Maidashi, Higashi-ku, Fukuoka, Fukuoka 812-8582, Japan

Edited by George N. DeMartino

The ubiquitin-proteasome system regulates the abundance of many cellular proteins by mediating their targeted degradation. We previously developed a method— differential proteomics– based identification of ubiquitylation substrates (DiPIUS)—for the comprehensive identification of substrates for a given F-box protein subunit of SCF-type ubiquitin ligases. We have now applied DiPIUS to the F-box protein Fbxw7 in three cell lines (mHepa, Neuro2A, and C2C12) and thereby identified myelin regulatory factor (MyRF), an endoplasmic reticulum–anchored transcription factor that is essential for myelination of nerves in the central nervous system, as a candidate substrate of Fbxw7 specifically in mHepa cells. Co-immunoprecipitation analysis confirmed that the NH$_2$-terminal cytoplasmic domain of MyRF interacted with Fbxw7 in these cells. Furthermore, an *in vitro* ubiquitylation assay revealed that MyRF undergoes polyubiquitylation in the presence of purified recombinant SCF^{Fbxw7}. In addition, the stability of MyRF in mHepa cells was increased by mutation of a putative phosphodegron sequence or by exposure of the cells to an inhibitor of glycogen synthase kinase-3 (GSK-3). We found that MyRF mRNA is not restricted to the central nervous system but is instead distributed widely among mouse tissues. Furthermore, with the use of RNA sequencing in mHepa cells overexpressing or depleted of MyRF, we identified many novel potential target genes of MyRF. Our results thus suggest that Fbxw7 controls the transcription of MyRF target genes in various tissues through regulation of MyRF protein stability in a manner dependent on MyRF phosphorylation by GSK-3.

The ubiquitin-proteasome system mediates the degradation of many cellular proteins with high specificity and plays an essential role in most cellular processes (1). The ubiquitylation cascade is mediated by three enzymes: a ubiquitin-activating enzyme (E1), a ubiquitin-conjugating enzyme (E2), and a ubiq-

uitin ligase (E3), with substrate specificity being determined by the E3 (2). The Skp1–Cul1–F-box protein (SCF) complex is one of the most well-characterized types of ubiquitin ligase. Each SCF complex is composed of four subunits: Skp1, Cul1, Rbx1, and an F-box protein (3–5). F-box proteins are responsible for substrate recognition by each complex and constitute a large family of >70 eukaryotic proteins (6). The relation between each F-box protein and its corresponding substrates has been largely unclear, however. We recently developed a new method, termed differential proteomics– based identification of ubiquitylation substrates (DiPIUS) (7), for the comprehensive identification of substrates for a given F-box protein. In the present study, we have applied DiPIUS to the F-box protein Fbxw7 (F-box and WD repeat domain– containing 7).

Fbxw7 was initially identified by genetic analysis as a negative regulator of LIN-12 (Notch)–mediated signaling in *Caenorhabditis elegans* (8, 9). It was subsequently shown to play a pivotal role in the control of cell proliferation through ubiquitylation of cyclin E (10 –13), c-Myc (13–15), Notch (9, 16, 17), c-Jun (18, 19), and Krüppel-like factor 5 (KLF5) (20, 21). Furthermore, Fbxw7 has recently been shown to contribute to cell differentiation and development. The loss of Fbxw7 in neural stem cells thus impairs their differentiation into neurons as a result of the up-regulation of Notch (22, 23). In addition, conditional ablation of Fbxw7 in the liver of mice results in a shift in the differentiation of liver stem cells from the hepatocyte lineage to cholangiocytes as well as in increased cell proliferation (24). Liver-specific loss of Fbxw7 also elicits lipid buildup in hepatocytes as a consequence of the accumulation of sterol response element– binding proteins (SREBPs), which are also substrates of Fbxw7 (24 –27). Depletion of Fbxw7 in C2C12 mesenchymal cells promotes their differentiation into osteoblasts in association with the accumulation of OASIS (28), whereas conditional ablation of Fbxw7 in primary mouse mesenchymal cells results in up-regulation of BBF2H7 and promotes chondrogenesis (28). SREBPs, OASIS, and BBF2H7 are all endoplasmic reticulum (ER)[2]–anchored transcription factors, with the NH$_2$-terminal domain of these proteins undergoing cleavage and trans-

[2] The abbreviations used are: ER, endoplasmic reticulum; DiPIUS, differential proteomics-based identification of ubiquitylation substrates; MyRF, myelin regulatory factor; ICD, intramolecular chaperone domain; CPD, Cdc4 phosphodegron; BIO, 6-bromoindirubin-3′-oxime; OPC, oligodendrocyte progenitor cell; FPKM, fragments per kilobase of exon per million mapped reads.

location to the nucleus, where it triggers the transactivation of target genes and thereby promotes specific cellular differentiation. Fbxw7 is thus implicated in the control of such ER-anchored transcription factors in addition to plasma membrane–anchored Notch.

Myelin regulatory factor (MyRF) is another ER membrane–anchored transcription factor and undergoes intramolecular chaperone domain (ICD)–mediated autocleavage that results in the separation of its nucleus-targeted NH_2-terminal region (MyRF(N)) from the COOH-terminal region containing the transmembrane domain (29). MyRF was first identified as the product of a gene expressed specifically by postmitotic oligodendrocytes in the CNS (30, 31). MyRF(N) binds to the *cis*-regulatory elements of multiple oligodendrocyte-specific genes related to myelination such as those for myelin basic protein, proteolipid protein 1 (PLP1), and myelin-associated glycoprotein. Conditional ablation of MyRF in the oligodendrocyte lineage of mice results in severe CNS dysmyelination and pronounced deficits in myelin gene expression (31). Inducible ablation of MyRF in mature oligodendrocytes of adult mice also results in a rapid down-regulation of myelin gene expression followed by a gradual degeneration of CNS myelin (32). These observations thus suggest that MyRF plays a central role in myelination in the CNS.

Unexpectedly, we found that MyRF is widely expressed in many tissues and cell types outside the CNS. Although many transcriptional targets of MyRF in the CNS have been identified and characterized, the roles of MyRF in other tissues are unknown. Here we show that Fbxw7 mediates the ubiquitylation of MyRF and controls its stability in mHepa mouse hepatocellular carcinoma cells. In addition, we identified many candidate target genes for MyRF by RNA sequencing in mHepa cells. Our results suggest that Fbxw7 regulates the abundance of MyRF and thereby plays unidentified roles outside the CNS.

Results

Identification of substrates for SCF^{Fbxw7} by DiPIUS

To comprehensively identify the substrates targeted by a given F-box protein for degradation, we previously developed a differential proteomics approach termed DiPIUS (7). The DiPIUS system is based on a difference in binding affinity for substrates between WT and mutant F-box proteins. Whereas WT F-box proteins bind weakly to their substrates, with such binding being followed by substrate ubiquitylation and degradation, F-box proteins with an inactivating mutation in the F-box domain are expected to associate more stably with substrates and thereby to allow their accumulation in the cell (Fig. 1A).

Both WT Fbxw7α (an alternatively spliced isoform of Fbxw7) and a mutant form of the protein lacking the entire F-box domain (ΔF mutant) were tagged at the NH_2 terminus with the FLAG epitope and expressed separately in mHepa, Neuro2A (mouse neuroblastoma), and C2C12 (mouse myoblast) cells. Cell lysates were subjected to immunoprecipitation with antibodies to FLAG, and the immunoprecipitated proteins were analyzed by LC-MS/MS. The abundance of proteins that bound to the WT or mutant forms of Fbxw7α was compared by semi-
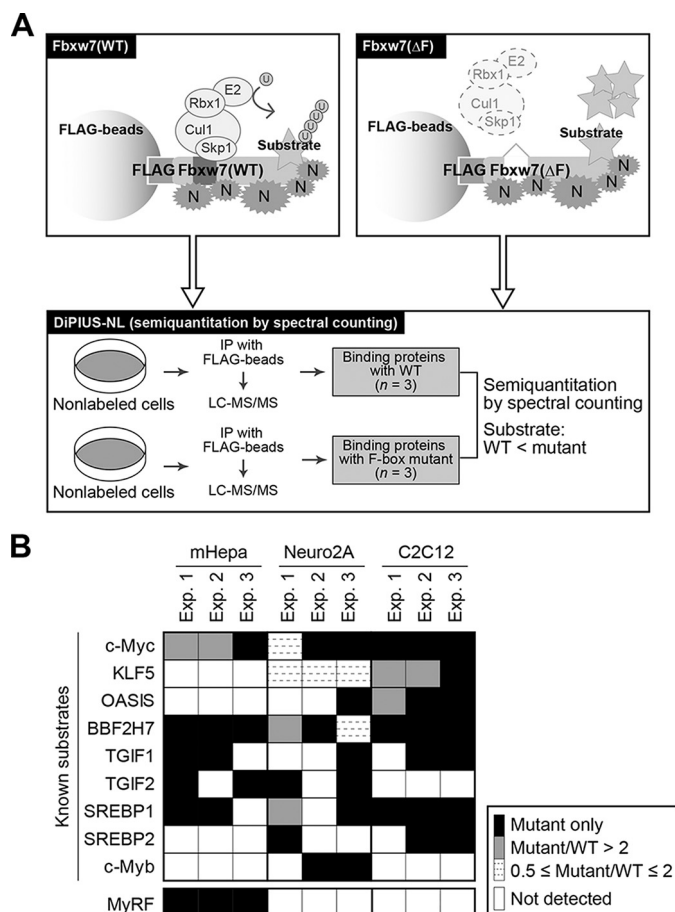

Figure 1. Identification of MyRF as a candidate substrate of SCF$^{Fbxw7\alpha}$ by DiPIUS. *A*, schematic representation of the comprehensive identification of substrates for Fbxw7. Proteins that bind to FLAG-tagged WT or ΔF mutant forms of Fbxw7α in transfected cells are analyzed by semiquantitative spectral counting (DiPIUS-NL). *U*, ubiquitin; *N*, nonspecific binding protein; *IP*, immunoprecipitation. *B*, the abundance of proteins that bound to Fbxw7α(WT) or Fbxw7α(ΔF) in the indicated cell lines and in three independent experiments (*Exp.*) was compared by semiquantitative spectral counting (these data are the same as those presented previously (28)). Proteins with a mutant/WT ratio of > 2 in at least two of three independent experiments, including known substrates of SCF$^{Fbxw7\alpha}$ as well as MyRF, are indicated. The ratios of the number of spectral counts for mutant and WT F-box proteins are indicated by the scale.

quantitative spectral counting (DiPIUS-NL) (Fig. 1A). We identified MyRF as a candidate substrate of Fbxw7α with the DiPIUS-NL system in mHepa cells but not in Neuro2A or C2C12 cells (Fig. 1B). We also identified an additional 18 potential novel substrates for Fbxw7 in one or more of these three cell lines.

The NH$_2$-terminal domain of MyRF interacts with Fbxw7

We verified the interaction between Fbxw7α and MyRF in mHepa cells with a co-immunoprecipitation assay. The full-length form of MyRF localized in the ER undergoes ICD-mediated autocleavage (29). The released MyRF(N) fragment then undergoes translocation to the nucleus, where Fbxw7α is localized (33, 34), and activates transcription of its target genes. Co-immunoprecipitation analysis revealed that the nuclear form of MyRF (MyRF(N)) was indeed associated to a greater extent with Fbxw7α(ΔF) than with Fbxw7α(WT) in mHepa cells, whereas the full-length form of MyRF (MyRF(FL)) did not
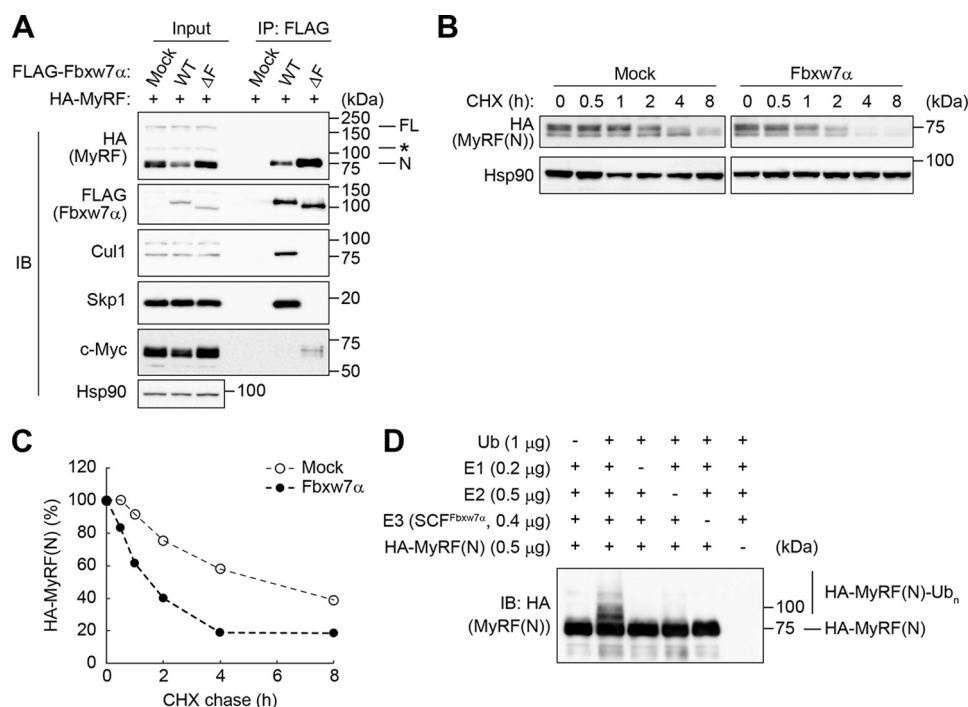
Figure 2. SCF$^{Fbxw7\alpha}$ ubiquitylates MyRF. *A*, co-immunoprecipitation of HA-tagged MyRF as well as of Cul1, Skp1, and c-Myc with FLAG-tagged WT or ΔF mutant forms of Fbxw7α from mHepa cell lysates. Immunoprecipitates (*IP*) prepared with antibodies to FLAG from cells expressing the recombinant Fbxw7α proteins (or from those transfected with the corresponding empty vector, Mock), as well as the original cell lysates (*Input*), were subjected to immunoblot (*IB*) analysis with antibodies to HA, to FLAG, or to the indicated proteins. Hsp90 was examined as a loading control. *FL*, *N*, and the *asterisk* indicate full-length and nuclear forms of MyRF as well as a nonspecific band, respectively. *B*, cycloheximide chase analysis of MyRF in mHepa cells stably expressing HA-tagged MyRF with or without Fbxw7α. Cells incubated with cycloheximide (*CHX*) (100 μg/ml) for the indicated times were subjected to immunoblot analysis with antibodies to HA. *C*, the percentage of HA-tagged MyRF(N) remaining after the various chase times in *B* was quantitated with ImageJ software. *D*, HA-tagged MyRF(N) (amino acids 1–586 of MyRF) was subjected to an *in vitro* ubiquitylation assay with immunopurified SCF$^{Fbxw7\alpha}$ and ATP as well as with E1, E2, and ubiquitin (*Ub*), as indicated. Reaction mixtures (10 μl) were subjected to immunoblot analysis with antibodies to HA. The positions of unmodified and polyubiquitylated (*Ub$_n$*) forms of MyRF(N) are indicated.

interact with Fbxw7α (Fig. 2*A*). These results suggested that the NH$_2$-terminal domain of MyRF encounters Fbxw7α in the nucleus, and that Fbxw7α might attenuate the function of MyRF to prevent excessive transactivation of its target genes.

Fbxw7 controls the stability of MyRF

We found that the ectopic expression of Fbxw7α(WT) reduced the amount of MyRF(N), but not that of MyRF(FL), in mHepa cells (Fig. 2*A*). Fbxw7α(ΔF), which lacks ubiquitylation activity, did not show such an effect, suggesting that Fbxw7α regulates the abundance of MyRF(N) in a ubiquitin-dependent manner. Cycloheximide chase analysis revealed that the half-life of MyRF(N) was indeed reduced by forced expression of Fbxw7α(WT) (Fig. 2, *B* and *C*).

We also examined whether MyRF is a direct substrate of SCF$^{Fbxw7\alpha}$ *in vitro*. MyRF(N) tagged with His$_6$ and HA epitopes was expressed in and purified from Sf21 insect cells with nickel-nitrilotriacetic acid (Ni-NTA) beads. Skp1 and Cul1 each tagged with the His$_6$ and Myc epitopes, Myc-tagged Rbx1, and His$_6$-FLAG–tagged Fbxw7α were also expressed in Sf21 cells and purified as the assembled SCF$^{Fbxw7\alpha}$ complex with antibodies to FLAG. An *in vitro* ubiquitylation assay with these recombinant proteins revealed that the ubiquitylation of MyRF(N) was apparent only in the presence of all reaction components, including Uba1 (E1), UbcH5C (E2), SCF$^{Fbxw7\alpha}$ (E3), and ubiquitin (Fig. 2*D*). Collectively, these results suggested that SCF$^{Fbxw7\alpha}$ is a *bona fide* ubiquitin ligase for MyRF(N).

CPD phosphorylation is required for recognition of MyRF by Fbxw7

Most substrates of Fbxw7 contain a conserved amino acid sequence for phosphorylation, termed the Cdc4 phosphodegron (CPD) (5). MyRF contains four potential CPD sequences (Fig. 3*A*). Given that three of these sequences are located in the nuclear translocation region of MyRF, we introduced mutations into these three motifs to examine which one is essential for the Fbxw7-mediated degradation of MyRF(N). Co-immunoprecipitation analysis revealed that a mutant (S138A/S142A) form of MyRF in which both Ser^{138} and Ser^{142} in the second CPD were replaced with alanine did not interact with Fbxw7α(ΔF) (Fig. 3*B*). Furthermore, cycloheximide chase analysis revealed that this mutant was more stable than WT or other CPD mutant proteins in mHepa cells (Fig. 3, *C* and *D*). Given that many CPDs of Fbxw7 substrates are phosphorylated by glycogen synthase kinase-3 (GSK-3) (5), we examined the stability of MyRF(N) in the presence of the GSK-3 inhibitor 6-bromoindirubin-3′-oxime (BIO). Cycloheximide chase analysis revealed that BIO treatment prolonged the half-life of MyRF(N) from 53 to 116 min (Fig. 3, *E* and *F*). In addition, the S138A/S142A mutant form of MyRF(N) did not undergo ubiquitylation *in vitro* (Fig. 3*G*). Together, these results thus indicated that the GSK-3–dependent phosphorylation of Ser^{138} and Ser^{142} in MyRF(N) is required for recognition and subsequent ubiquitylation by SCF^{Fbxw7}.
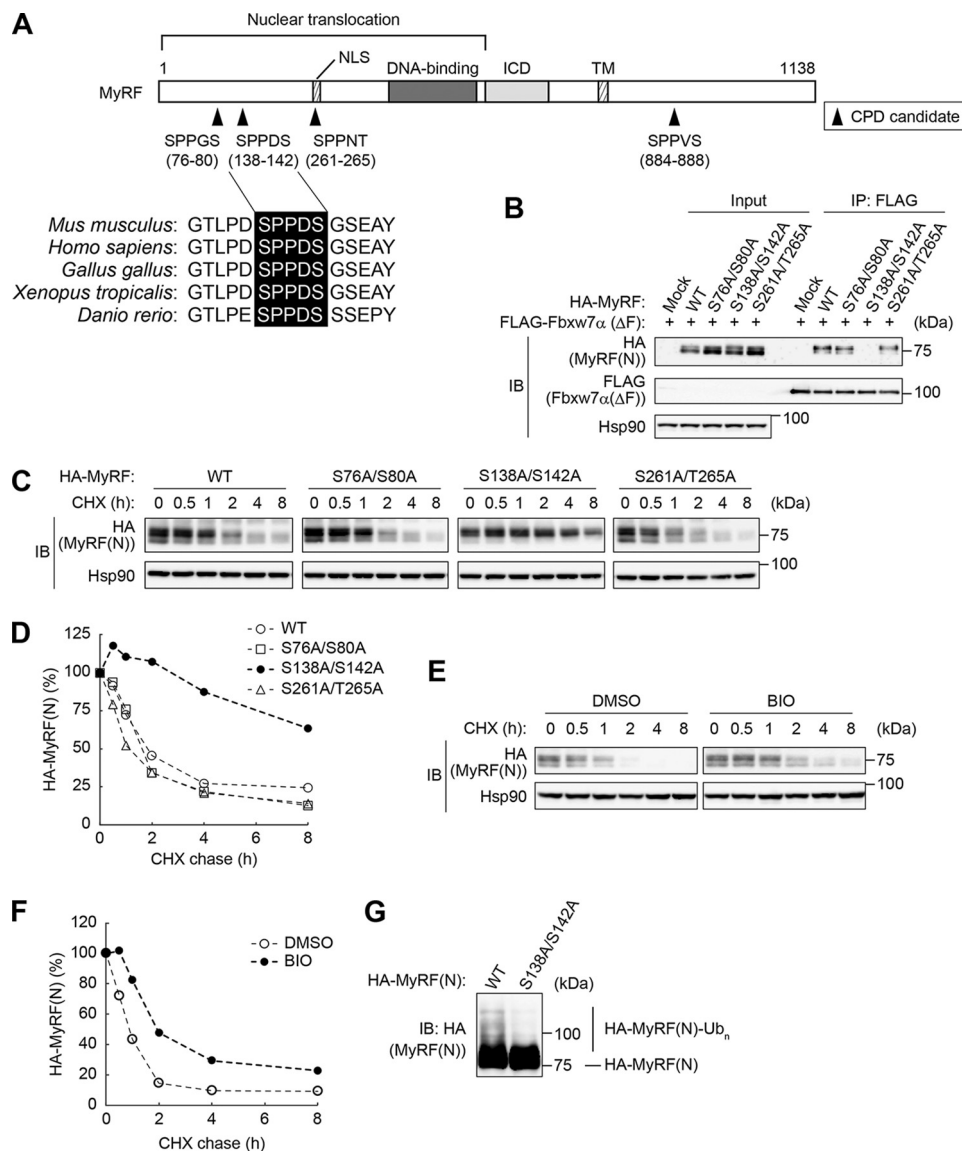
Figure 3. CPD phosphorylation is required for ubiquitylation of MyRF. *A*, domain organization of mouse MyRF. Four potential CPD sequences as well as the nuclear localization sequence (*NLS*), DNA-binding domain, intramolecular chaperone domain (*ICD*), and transmembrane domain (*TM*) are shown. The second CPD sequence is fully conserved among the indicated vertebrate species. *B*, effects of CPD mutation on the binding of MyRF(N) to Fbxw7α(ΔF). Lysates of mHepa cells expressing FLAG-tagged Fbxw7α(ΔF) as well as HA-tagged forms of MyRF or its CPD mutants were subjected to immunoprecipitation with antibodies to FLAG, and the resulting precipitates as well as the original cell lysates were subjected to immunoblot analysis with antibodies to HA and to FLAG. *C* and *E*, cycloheximide chase analysis of MyRF(N) in mHepa cells. Cells stably expressing WT or CPD mutant forms of HA-tagged MyRF (*C*) or those expressing HA-MyRF(WT) (*E*) were incubated for the indicated times in the presence of cycloheximide (100 μg/ml) either without (*C*) or with 1 μM BIO or DMSO vehicle (*E*). Cell lysates were then subjected to immunoblot analysis with antibodies to HA. *D* and *F*, the percentage of HA-tagged forms of MyRF(N) remaining after the various chase times in *C* and *E*, respectively, was quantitated with ImageJ software. *G*, HA-tagged MyRF(N) (amino acids 1–586 of MyRF) or its indicated CPD mutant was subjected to an *in vitro* ubiquitylation assay with immunopurified SCF$^{Fbxw7\alpha}$, ATP, E1, E2, and ubiquitin. Reaction mixtures (10 μl) were subjected to immunoblot analysis with antibodies to HA. The positions of unmodified and polyubiquitylated (Ub$_n$) forms of MyRF(N) are indicated.

Fbxw7 restrains oligodendrocyte maturation

We found that depletion of Fbxw7 in mouse oligodendrocyte progenitor cells (OPCs) by shRNA-mediated RNAi promoted the differentiation of these cells into mature oligodendrocytes. Expression of the genes for the oligodendrocyte marker proteins PLP1 and 2′,3′-cyclic nucleotide-3′-phosphodiesterase (CNP), both of which are target genes of MyRF, was thus up-regulated in OPCs depleted of Fbxw7 compared with those expressing a control shRNA (Fig. 4). In contrast, expression of the gene for the OPC marker platelet-derived growth factor receptor α (PDGFRα) (31) was attenuated by Fbxw7 depletion. These results suggested that Fbxw7 depletion leads to the accumulation of MyRF(N) in OPCs and thereby promotes their maturation into oligodendrocytes.

Identification of novel candidate target genes of MyRF

It was unexpected that we identified MyRF as a target of Fbxw7 in mHepa cells, given that most previous studies of MyRF have focused on its role in the CNS. To investigate the distribution of MyRF mRNA, we performed RT and real-time PCR analysis of mouse tissues. MyRF mRNA was detected not only in the CNS but in all tissues examined with the exception of quadriceps and bone marrow (Fig. 5), suggesting that MyRF might have other unrecognized roles in
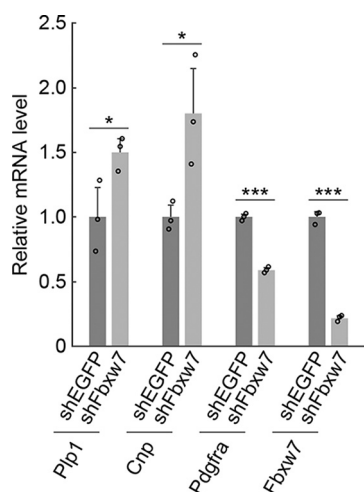
Figure 4. Effects of Fbxw7 knockdown on gene expression in OPCs. The abundance of mRNAs for the indicated genes was determined by RT and real-time PCR analysis in OPCs expressing Fbxw7 (*shFbxw7*) or control (*shEGFP*) shRNAs. Data were normalized by the amount of *Rps18* mRNA, are expressed relative to the corresponding control value, and are mean ± S.D. from three independent experiments, with the values from individual experiments being indicated by *circles*. *, $p < 0.05$, ***, $p < 0.001$ (Student's *t* test).

addition to transactivation of myelin-associated genes in the CNS.

To investigate possible roles of MyRF outside of the CNS, we performed RNA sequencing in mHepa cells to identify novel genes that might be targeted by MyRF. RNA samples from mHepa cells engineered to overexpress or to be depleted of MyRF were purified and used to prepare RNA libraries for analysis with the HiSeq 1500 system (Illumina) and calculation of FPKM (fragments per kilobase of exon per million mapped reads) values. We identified 39 genes as positively regulated by MyRF (overlap of 1321 genes that were up-regulated by MyRF overexpression and 174 genes that were down-regulated by MyRF knockdown) (Fig. 6A). Conversely, 33 genes were negatively regulated by MyRF (overlap of 1737 genes that were down-regulated by MyRF overexpression and 113 genes that were up-regulated by MyRF knockdown) (Fig. 6B). We confirmed by RT and real-time PCR analysis that the amounts of mRNAs for *4930486L24Rik*, *Gm5549*, and *Hpgds*, the genes revealed by RNA sequencing to be most up-regulated by MyRF overexpression, were indeed increased in mHepa cells overexpressing MyRF (Fig. 6C). We also verified by RT and real-time PCR analysis that the expression levels of *Fam46a*, *Col14a1*, and *Akr1c18*, the genes most down-regulated by MyRF overexpression, were reduced in mHepa cells overexpressing MyRF (Fig. 6D). Together, these data suggested that MyRF is expressed and plays unidentified roles in tissues outside of the CNS.

Discussion

With the use of the DiPIUS system, we have identified MyRF as a novel substrate of Fbxw7α. A series of validation assays confirmed that the nucleus-targeted NH$_2$-terminal region of MyRF is a *bona fide* substrate of Fbxw7α. Consistent with our findings, a mutation that disrupts the *Fbxw7* ortholog in zebrafish was shown to elicit hypermyelination (35), possibly as a result of the accumulation of MyRF in oligodendrocytes

because of its impaired degradation. Further studies will be required to confirm a role for Fbxw7 in myelination in mammals.

Fbxw7α mediates the nuclear degradation of many transcription factors, some of which are localized at the ER membrane under basal conditions but undergo cleavage and translocation to the nucleus in response to specific cues. SREBPs are such ER-anchored transcription factors that are cleaved in response to a reduction in the intracellular level of cholesterol, with the mature form of these proteins being translocated to the nucleus to mediate activation of lipogenesis. OASIS and BBF2H7 are also ER-anchored transcription factors that are cleaved in response to ER stress and promote osteogenesis and chondrogenesis, respectively. MyRF undergoes autocleavage and promotes myelination. Fbxw7α targets the nuclear forms of all of these transcription factors (SREBPs, OASIS, BBF2H7, and MyRF). Fbxw7 was originally discovered as a regulator of Notch (8, 9), which is also a membrane-anchored transcription factor that undergoes cleavage, with the COOH-terminal intracellular domain of this protein being translocated to the nucleus and there activating downstream target genes to induce cellular differentiation. Fbxw7 might thus function to extinguish the transactivation activity of these various transcription factors in the nucleus, thereby contributing to the strict regulation of transcription by membrane-anchored transcription factors (Fig. 7).

We found that MyRF mRNA is not restricted to the CNS but is instead widely distributed among mouse tissues. We identified many candidates for target genes of MyRF in mHepa cells by RNA sequencing. Among the candidate genes positively regulated by MyRF, *Ngef* (encoding Ephexin-1) and *Ctgf* (which encodes connective tissue growth factor and is also known as *Ccn2*, *Fisp12*, or *Hcs24*) contribute to maturation of the neuromuscular junction (36, 37) and to angiogenesis (38, 39), chondrogenesis (38), and pancreas development (40), respectively. On the other hand, *Apela* (also known as *Ela*, *Ende*, *Gm10664*, or *Tdl*) and *Traf5*, two of the genes negatively regulated by MyRF, have been shown to contribute to heart development (41) and mesendodermal cell movement during gastrulation (42) and to osteoclastogenesis (43), respectively. Collectively, these observations suggest that MyRF might function to orchestrate developmental programs outside the CNS. Fbxw7 might thus contribute to the control of developmental processes as an upstream regulator of the stability of MyRF as well as that of other ER-anchored transcription factors including SREBPs, OASIS, and BBF2H7.

Experimental procedures

Mice

WT C57BL/6J mice were obtained from CLEA Japan (Tokyo). Mouse experiments were approved by the Animal Ethics Committee of Kyushu University.

Cell culture

mHepa, Neuro2A, and C2C12 cells were maintained at 37 °C in DMEM supplemented with 10% FBS (Invitrogen), 1 mM sodium pyruvate, penicillin (100 units/ml) (Invitrogen), streptomycin (100 mg/ml) (Invitrogen), 2 mM L-glutamine, and non-
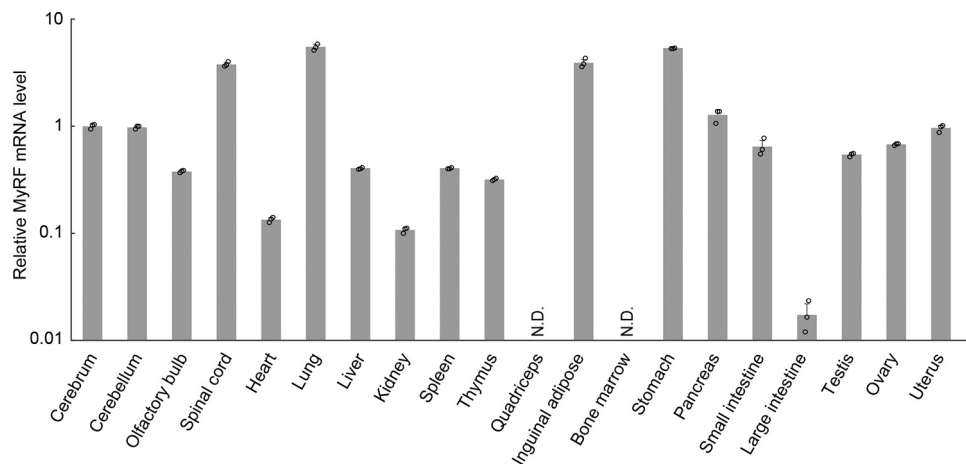
Figure 5. Tissue distribution of MyRF mRNA. The abundance of MyRF mRNA in the indicated mouse tissues was determined by RT and real-time PCR analysis. Data were normalized by the amount of *Gapdh* mRNA, are expressed relative to the value for cerebrum, and are mean ± S.D. from three independent experiments, with the values from individual experiments being indicated by *circles*. *N.D.*, not detected.
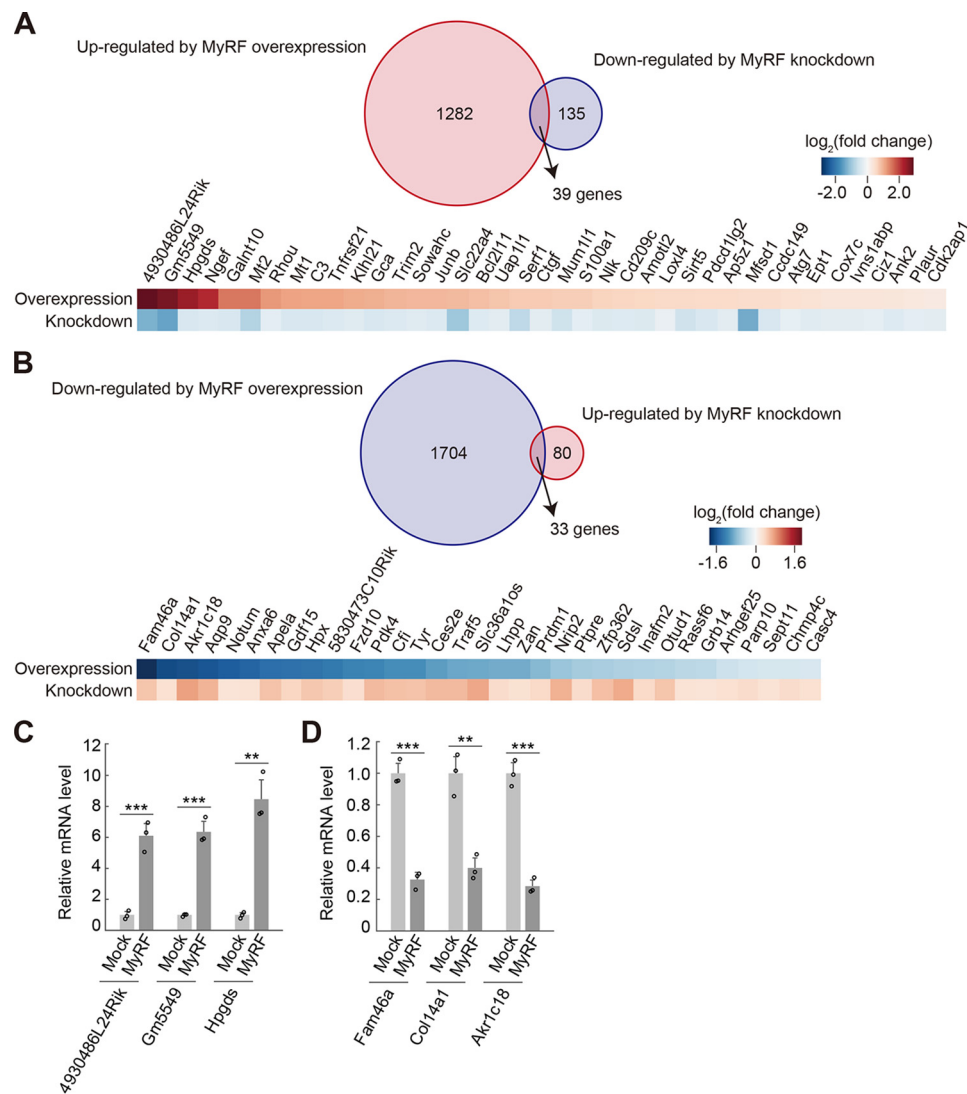

Figure 6. Identification of potential novel target genes of MyRF. *A* and *B*, Venn diagrams for overlap of genes whose expression in mHepa cells was revealed by RNA sequencing to be up-regulated by MyRF overexpression or down-regulated by MyRF knockdown (*A*) or to be down-regulated by MyRF overexpression or up-regulated by MyRF knockdown (*B*). The false discovery rate (FDR, q-score) cutoff value was set as 0.05. The heatmap shows log$_2$(-fold change in FPKM) for each gene. *C* and *D*, RT and real-time PCR analysis of mRNA abundance for the indicated genes in mHepa cells overexpressing (or not, Mock) MyRF. Data were normalized by the amount of *Rps18* mRNA, are expressed relative to the corresponding control value, and are mean ± S.D. from three independent experiments, with the values from individual experiments being indicated by *circles*. **, $p < 0.01$; ***, $p < 0.001$ (Student's *t* test).
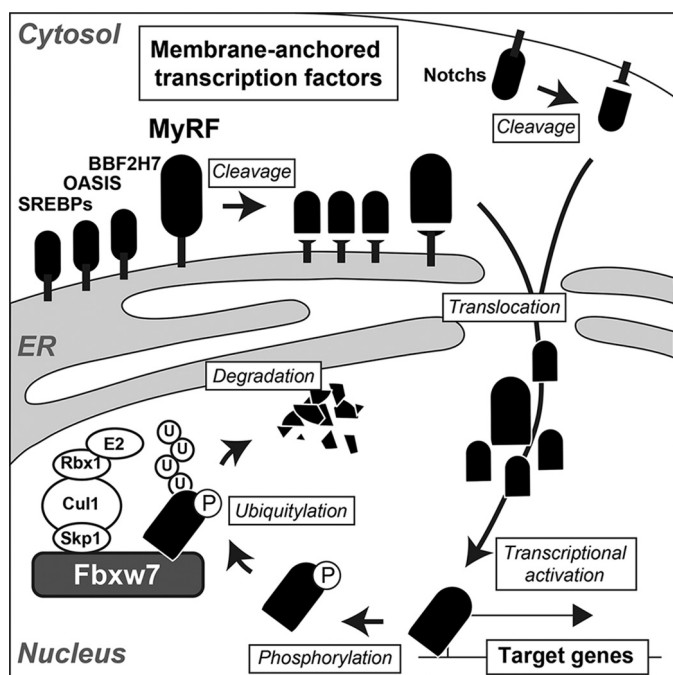
Figure 7. Model for Fbxw7-mediated regulation of the abundance of membrane-anchored transcription factors. ER-anchored transcription factors (MyRF, BBF2H7, OASIS, and SREBPs) and plasma membrane–anchored transcription factors (Notch proteins) are cleaved to release fragments that undergo translocation to the nucleus, where they activate target genes. The nuclear forms of these proteins are phosphorylated, ubiquitylated by SCF^{Fbxw7}, and thereby targeted for degradation by the proteasome, thus preventing excessive transactivation of target genes. *U*, ubiquitin; *P*, phosphate.

essential amino acids (10 ml/liter) (Invitrogen). Sf21 cells were cultured at 27 °C in Sf-900 II serum-free medium (SFM) (Invitrogen) supplemented with 5% FBS (Invitrogen), penicillin (100 units/ml) (Invitrogen), and streptomycin (100 mg/ml) (Invitrogen). Primary OPCs were isolated from the cerebral cortex of mice at postnatal day 7 by immunopanning as described previously (44), with minor modifications. In brief, the tissue was incubated for 20 min at 37 °C with 0.25% trypsin-EDTA and was then subjected to gentle dissociation after the addition of DMEM supplemented with 10% FBS and DNase (10 mg/ml). The dissociated cells were incubated for 45 min at room temperature in dishes coated with antibodies to PDGFRα, nonadherent cells were removed by washing, and OPCs bound to the dishes were collected by exposure to 0.25% trypsin-EDTA. The OPCs were cultured at 37 °C in OPC medium consisting of Neurobasal Medium (Invitrogen) supplemented with B-27 Supplement (20 ml/liter) (Invitrogen), 2 mM L-glutamine, nonessential amino acids (10 ml/liter) (Invitrogen), recombinant mouse basic fibroblast growth factor (40 ng/ml) (R&D Systems, Minneapolis, MN), and recombinant human PDGF-AA (20 ng/ml) (PeproTech, Rocky Hill, NJ).

Antibodies

Antibodies to the FLAG epitope (M2) were obtained from Sigma; those to the HA epitope (HA.11 or Y-11) from Covance (Princeton, NJ) or Santa Cruz Biotechnology (Dallas, TX), respectively; those to Skp1, to Hsp90, and to CD140a (PDGFRα) from BD Biosciences; those to Cul1 from Cell Signaling Technology (Danvers, MA); and those to c-Myc from

Abcam. HRP-conjugated goat antibodies to mouse or rabbit IgG were obtained from Promega (Madison, WI).

Plasmids

Complementary DNAs encoding mouse Fbxw7α or its ΔF mutant were subcloned into p3×FLAG-CMV 7.1 (Sigma), and those for HA epitope–tagged mouse MyRF or its mutants were subcloned into pcDNA3 (Invitrogen). The resulting vectors were introduced into mHepa cells with the use of the Lipofectamine 2000 transfection reagent (Invitrogen) for transient expression. For retroviral expression, cDNAs for FLAG epitope–tagged mouse Fbxw7α or for HA epitope–tagged mouse MyRF, or shRNA expression cassettes (mouse U6 gene promoter and each target sequence for mouse MyRF or mouse Fbxw7) were subcloned into pMX-puro (kindly provided by T. Kitamura). The resulting vectors were introduced into Plat E cells with the use of the X-tremeGENE 9 DNA transfection reagent (Roche), and recombinant retroviruses released into culture supernatants were used to infect mHepa cells or primary OPCs. The infected cells were subjected to selection in medium containing puromycin (6 μg/ml). For baculoviral expression, cDNAs for FLAG-tagged mouse Fbxw7α, HA epitope–tagged mouse MyRF(N), and Myc epitope–tagged mouse Cul1 and Skp1 were subcloned into pFASTBac HT (encoding a His$_6$ tag), whereas that for human Rbx1 containing an NH$_2$-terminal Myc epitope tag was subcloned into pFASTBac1 (Invitrogen).

DiPIUS-NL

DiPIUS-NL was performed in mHepa, Neuro2A, and C2C12 cells as described previously (7, 28). All data are available in ProteomeXchange and jPOSTrepo (45) under the accession numbers PXD008705 and JPST000373, respectively.

Cycloheximide chase analysis, GSK-3 inhibitor treatment, immunoprecipitation, and immunoblot analysis

For cycloheximide chase experiments, cycloheximide (100 μg/ml) was added to culture medium and the cells were harvested at the indicated times thereafter. For GSK-3 inhibition, cells were cultured in the presence of 1 μM BIO for 1 h before the addition of cycloheximide. Cells were lysed as described previously (46). Immunoprecipitation and immunoblot analysis were also performed as described previously (47), with Hsp90 as a loading control and immunoblot intensity quantitated with ImageJ software.

In vitro ubiquitylation assay

An *in vitro* ubiquitylation assay was performed as described previously (48). Recombinant baculoviruses encoding His$_6$-FLAG-Fbxw7α, His$_6$-Myc-Cul1, His$_6$-Myc-Skp1, Myc-Rbx1, and His$_6$-HA-MyRF(N) were generated with the Bac-to-Bac baculovirus system (Invitrogen) (49). Recombinant SCF^{Fbxw7α} and HA-MyRF(N) were purified for the *in vitro* ubiquitylation assay as described previously (28).

RNAi

Construction of shRNA vectors was performed as described previously (50). The sequence targeted for mouse MyRF was

5′-GCCCAAATGCTGAACGGAATG-3′, and that for mouse Fbxw7 was 5′-GGACAGTGTTTACAAACTTTG-3′. An shRNA vector for enhanced GFP (EGFP) was used as a control.

RT and real-time PCR analysis

Total RNA isolated from cells or various mouse tissues with the use of Isogen (Nippon Gene, Tokyo, Japan) was subjected to RT with a QuantiTect Reverse Transcription Kit (Qiagen, Valencia, CA). The resulting cDNA was subjected to real-time PCR analysis with SYBR Green PCR Master Mix (TaKaRa, Shiga, Japan) and specific primers in a StepOnePlus real-time PCR system (Applied Biosystems, Foster City, CA). The sequences of the various primers (mouse sense and antisense, respectively) were 5′-CTGGCTGAGGGCTTCTACAC-3′ and 5′-GACTGACAGGTGGTCCAGGT-3′ for *Plp1*, 5′-CATCC-TCAGGAGCAAAGGAG-3′ and 5′-GTACGCCTCGGAGA-AGTCTG-3′ for *Cnp*, 5′-TATCCTCCCAAACGAGAATG-AGA-3′ and 5′-GTGGTTGTAGTAGCAAGTGTACC-3′ for *Pdgfra*, 5′-TGAAGTTCGTTCCTTTTCTTTGG-3′ and 5′-CAAAAGTTGTTGGTGTTGCTGAA-3′ for *Fbxw7*, 5′-AGC-CCAAGTACGTCAAGACA-3′ and 5′-CTGCTCAGGGG-GAAGATTGA-3′ for *Myrf*, 5′-CCACAGTGCAAAAGGGT-CCA-3′ and 5′-CAAGTGTAGCAATCCCGCAG-3′ for *4930486L24Rik*, 5′-TTGCCAGTCGCTTTGCTTAC-3′ and 5′-CCAGCAGAGCTTTTCCCACT-3′ for *Gm5549*, 5′-TGG-ACACGCTGGATGACTTC-3′ and 5′-GCCCAGGTTACAT-AATTGCCT-3′ for *Hpgds*, 5′-CCGAAGGGGTGAACAA-GGAG-3′ and 5′-GCCACTGTTGTTTGACAGGG-3′ for *Fam46a*, 5′-CTGAAGCACCCACAGCCATA-3′ and 5′-ACT-CCAGGCACCATAACCAC-3′ for *Col14a1*, 5′-TGAAGCCA-GGGAATGAGCTTT-3′ and 5′-TCATCTTGCAGTAGGCC-AGC-3′ for *Akr1c18*, 5′-AGGTTGTCTCCTGCGACTTCA-3′ and 5′-CCAGGAAATGAGCTTGACAAAGTT-3′ for *Gapdh*, and 5′-GAGGACCTGGAGAGGCTGAAG-3′ and 5′-CTGC-GGCCAGTGGTCTTG-3′ for *Rps18*. The amounts of target mRNAs were normalized by that of *Gapdh* or *Rps18* mRNA.

RNA sequencing and data analysis

RNA sequencing was performed as described previously (51). Total RNA was extracted from retrovirus-infected mHepa cells. Illumina libraries were constructed with the use of a NEB-Next Ultra Directional RNA Library Prep Kit for Illumina. Single-end reads were mapped to mm10 (UCSC) with TopHat (v2.1.1) and the mm10 GTF file. Data were processed with the Linux system for calculation of FPKM values with the use of Cuffdiff (v2.2.1) and the option "-N." Sequence data have been deposited in the DDBJ Sequence Read Archive under the accession number DRA005955.

Statistical analysis

Where indicated, quantitative data are presented as mean ± S.D. and were analyzed with Student's *t* test. A *p* value of < 0.05 was considered statistically significant.

References

1. Hershko, A., and Ciechanover, A. (1998) The ubiquitin system. *Annu. Rev. Biochem.* **67,** 425– 479 CrossRef Medline
2. Pickart, C. M., and Eddins, M. J. (2004) Ubiquitin: structures, functions, mechanisms. *Biochim. Biophys. Acta* **1695,** 55–72 CrossRef Medline
3. Nakayama, K. I., and Nakayama, K. (2006) Ubiquitin ligases: Cell-cycle control and cancer. *Nat. Rev. Cancer* **6,** 369 –381 CrossRef Medline
4. Frescas, D., and Pagano, M. (2008) Deregulated proteolysis by the F-box proteins SKP2 and β-TrCP: Tipping the scales of cancer. *Nat. Rev. Cancer* **8,** 438 – 449 CrossRef Medline
5. Welcker, M., and Clurman, B. E. (2008) FBW7 ubiquitin ligase: A tumour suppressor at the crossroads of cell division, growth and differentiation. *Nat. Rev. Cancer* **8,** 83–93 CrossRef Medline
6. Jin, J., Cardozo, T., Lovering, R. C., Elledge, S. J., Pagano, M., and Harper, J. W. (2004) Systematic analysis and nomenclature of mammalian F-box proteins. *Genes Dev.* **18,** 2573–2580 CrossRef Medline
7. Yumimoto, K., Matsumoto, M., Oyamada, K., Moroishi, T., and Nakayama, K. I. (2012) Comprehensive identification of substrates for F-box proteins by differential proteomics analysis. *J. Proteome Res.* **11,** 3175–3185 CrossRef Medline
8. Sundaram, M., and Greenwald, I. (1993) Suppressors of a lin-12 hypomorph define genes that interact with both lin-12 and glp-1 in *Caenorhabditis elegans. Genetics* **135,** 765–783
9. Hubbard, E. J., Wu, G., Kitajewski, J., and Greenwald, I. (1997) sel-10, a negative regulator of *lin-12* activity in *Caenorhabditis elegans*, encodes a member of the CDC4 family of proteins. *Genes Dev.* **11,** 3182–3193 CrossRef Medline
10. Koepp, D. M., Schaefer, L. K., Ye, X., Keyomarsi, K., Chu, C., Harper, J. W., and Elledge, S. J. (2001) Phosphorylation-dependent ubiquitination of cyclin E by the SCF^Fbw7 ubiquitin ligase. *Science* **294,** 173–177 CrossRef Medline
11. Moberg, K. H., Bell, D. W., Wahrer, D. C., Haber, D. A., and Hariharan, I. K. (2001) Archipelago regulates cyclin E levels in *Drosophila* and is mutated in human cancer cell lines. *Nature* **413,** 311–316 CrossRef Medline
12. Strohmaier, H., Spruck, C. H., Kaiser, P., Won, K. A., Sangfelt, O., and Reed, S. I. (2001) Human F-box protein hCdc4 targets cyclin E for proteolysis and is mutated in a breast cancer cell line. *Nature* **413,** 316 –322 CrossRef Medline
13. Yokobori, T., Mimori, K., Iwatsuki, M., Ishii, H., Onoyama, I., Fukagawa, T., Kuwano, H., Nakayama, K. I., and Mori, M. (2009) p53-altered FBXW7 expression determines poor prognosis in gastric cancer cases. *Cancer Res.* **69,** 3788 –3794 CrossRef Medline
14. Yada, M., Hatakeyama, S., Kamura, T., Nishiyama, M., Tsunematsu, R., Imaki, H., Ishida, N., Okumura, F., Nakayama, K., and Nakayama, K. I. (2004) Phosphorylation-dependent degradation of c-Myc is mediated by the F-box protein Fbw7. *EMBO J.* **23,** 2116 –2125 CrossRef Medline
15. Welcker, M., Orian, A., Jin, J., Grim, J. E., Grim, J. A., Harper, J. W., Eisenman, R. N., and Clurman, B. E. (2004) The Fbw7 tumor suppressor regulates glycogen synthase kinase 3 phosphorylation-dependent c-Myc protein degradation. *Proc. Natl. Acad. Sci. U.S.A.* **101,** 9085–9090 CrossRef Medline
16. Gupta-Rossi, N., Le Bail, O., Gonen, H., Brou, C., Logeat, F., Six, E., Ciechanover, A., and Israël, A. (2001) Functional interaction between SEL-10, an F-box protein, and the nuclear form of activated Notch1 receptor. *J. Biol. Chem.* **276,** 34371–34378 CrossRef Medline
17. Oberg, C., Li, J., Pauley, A., Wolf, E., Gurney, M., and Lendahl, U. (2001) The Notch intracellular domain is ubiquitinated and negatively regulated

by the mammalian Sel-10 homolog. *J. Biol. Chem.* **276,** 35847–35853 CrossRef Medline

18. Nateri, A. S., Riera-Sans, L., Da Costa, C., and Behrens, A. (2004) The ubiquitin ligase SCF[Fbw7] antagonizes apoptotic JNK signaling. *Science* **303,** 1374–1378 CrossRef Medline

19. Wei, W., Jin, J., Schlisio, S., Harper, J. W., and Kaelin, W. G., Jr. (2005) The v-Jun point mutation allows c-Jun to escape GSK3-dependent recognition and destruction by the Fbw7 ubiquitin ligase. *Cancer Cell* **8,** 25–33 CrossRef Medline

20. Liu, N., Li, H., Li, S., Shen, M., Xiao, N., Chen, Y., Wang, Y., Wang, W., Wang, R., Wang, Q., Sun, J., and Wang, P. (2010) The Fbw7/human CDC4 tumor suppressor targets proproliferative factor KLF5 for ubiquitination and degradation through multiple phosphodegron motifs. *J. Biol. Chem.* **285,** 18858–18867 CrossRef Medline

21. Zhao, D., Zheng, H. Q., Zhou, Z., and Chen, C. (2010) The Fbw7 tumor suppressor targets KLF5 for ubiquitin-mediated degradation and suppresses breast cell proliferation. *Cancer Res.* **70,** 4728–4738 CrossRef Medline

22. Hoeck, J. D., Jandke, A., Blake, S. M., Nye, E., Spencer-Dene, B., Brandner, S., and Behrens, A. (2010) Fbw7 controls neural stem cell differentiation and progenitor apoptosis via Notch and c-Jun. *Nat. Neurosci.* **13,** 1365–1372 CrossRef Medline

23. Matsumoto, A., Onoyama, I., Sunabori, T., Kageyama, R., Okano, H., and Nakayama, K. I. (2011) Fbxw7-dependent degradation of Notch is required for control of "stemness" and neuronal-glial differentiation in neural stem cells. *J. Biol. Chem.* **286,** 13754–13764 CrossRef Medline

24. Onoyama, I., Suzuki, A., Matsumoto, A., Tomita, K., Katagiri, H., Oike, Y., Nakayama, K., and Nakayama, K. I. (2011) Fbxw7 regulates lipid metabolism and cell fate decisions in the mouse liver. *J. Clin. Invest.* **121,** 342–354 CrossRef Medline

25. Sundqvist, A., Bengoechea-Alonso, M. T., Ye, X., Lukiyanchuk, V., Jin, J., Harper, J. W., and Ericsson, J. (2005) Control of lipid metabolism by phosphorylation-dependent degradation of the SREBP family of transcription factors by SCF[Fbw7]. *Cell Metab.* **1,** 379–391 CrossRef Medline

26. Bengoechea-Alonso, M. T., and Ericsson, J. (2010) The ubiquitin ligase Fbxw7 controls adipocyte differentiation by targeting C/EBPα for degradation. *Proc. Natl. Acad. Sci. U.S.A.* **107,** 11817–11822 CrossRef Medline

27. Kumadaki, S., Karasawa, T., Matsuzaka, T., Ema, M., Nakagawa, Y., Nakakuki, M., Saito, R., Yahagi, N., Iwasaki, H., Sone, H., Takekoshi, K., Yatoh, S., Kobayashi, K., Takahashi, A., Suzuki, H., Takahashi, S., Yamada, N., and Shimano, H. (2011) Inhibition of ubiquitin ligase F-box and WD repeat domain-containing 7α (Fbw7α) causes hepatosteatosis through Krüppel-like factor 5 (KLF5)/peroxisome proliferator-activated receptor γ2 (PPARγ2) pathway but not SREBP-1c protein in mice. *J. Biol. Chem.* **286,** 40835–40846 CrossRef Medline

28. Yumimoto, K., Matsumoto, M., Onoyama, I., Imaizumi, K., and Nakayama, K. I. (2013) F-box and WD repeat domain-containing-7 (Fbxw7) protein targets endoplasmic reticulum-anchored osteogenic and chondrogenic transcriptional factors for degradation. *J. Biol. Chem.* **288,** 28488–28502 CrossRef Medline

29. Bujalka, H., Koenning, M., Jackson, S., Perreau, V. M., Pope, B., Hay, C. M., Mitew, S., Hill, A. F., Lu, Q. R., Wegner, M., Srinivasan, R., Svaren, J., Willingham, M., Barres, B. A., and Emery, B. (2013) MYRF is a membrane-associated transcription factor that autoproteolytically cleaves to directly activate myelin genes. *PLoS Biol.* **11,** e1001625 CrossRef Medline

30. Cahoy, J. D., Emery, B., Kaushal, A., Foo, L. C., Zamanian, J. L., Christopherson, K. S., Xing, Y., Lubischer, J. L., Krieg, P. A., Krupenko, S. A., Thompson, W. J., and Barres, B. A. (2008) A transcriptome database for astrocytes, neurons, and oligodendrocytes: A new resource for understanding brain development and function. *J. Neurosci.* **28,** 264–278 CrossRef Medline

31. Emery, B., Agalliu, D., Cahoy, J. D., Watkins, T. A., Dugas, J. C., Mulinyawe, S. B., Ibrahim, A., Ligon, K. L., Rowitch, D. H., and Barres, B. A. (2009) Myelin gene regulatory factor is a critical transcriptional regulator required for CNS myelination. *Cell* **138,** 172–185 CrossRef Medline

32. Koenning, M., Jackson, S., Hay, C. M., Faux, C., Kilpatrick, T. J., Willingham, M., and Emery, B. (2012) Myelin gene regulatory factor is required

33. Ye, X., Nalepa, G., Welcker, M., Kessler, B. M., Spooner, E., Qin, J., Elledge, S. J., Clurman, B. E., and Harper, J. W. (2004) Recognition of phosphodegron motifs in human cyclin E by the SCF[Fbw7] ubiquitin ligase. *J. Biol. Chem.* **279,** 50110–50119 CrossRef Medline

34. Welcker, M., Orian, A., Grim, J. E., Grim, J.A., Eisenman, R. N., and Clurman, B. E. (2004) A nucleolar isoform of the Fbw7 ubiquitin ligase regulates c-Myc and cell size. *Curr. Biol.* **14,** 1852–1857 CrossRef Medline

35. Kearns, C. A., Ravanelli, A. M., Cooper, K., and Appel, B. (2015) Fbxw7 limits myelination by inhibiting mTOR signaling. *J. Neurosci.* **35,** 14861–14871 CrossRef Medline

36. Sahin, M., Greer, P. L., Lin, M. Z., Poucher, H., Eberhart, J., Schmidt, S., Wright, T. M., Shamah, S. M., O'Connell, S., Cowan, C. W., Hu, L., Goldberg, J. L., Debant, A., Corfas, G., Krull, C. E., and Greenberg, M. E. (2005) Eph-dependent tyrosine phosphorylation of ephexin1 modulates growth cone collapse. *Neuron* **46,** 191–204 CrossRef Medline

37. Shi, L., Butt, B., Ip, F. C., Dai, Y., Jiang, L., Yung, W. H., Greenberg, M. E., Fu, A. K., and Ip, N. Y. (2010) Ephexin1 is required for structural maturation and neurotransmission at the neuromuscular junction. *Neuron* **65,** 204–216 CrossRef Medline

38. Ivkovic, S., Yoon, B. S., Popoff, S. N., Safadi, F. F., Libuda, D. E., Stephenson, R. C., Daluiski, A., and Lyons, K. M. (2003) Connective tissue growth factor coordinates chondrogenesis and angiogenesis during skeletal development. *Development* **130,** 2779–2791 CrossRef Medline

39. Hall-Glenn, F., De Young, R. A., Huang, B. L., van Handel, B., Hofmann, J. J., Chen, T. T., Choi, A., Ong, J. R., Benya, P. D., Mikkola, H., Iruela-Arispe, M. L., and Lyons, K. M. (2012) CCN2/connective tissue growth factor is essential for pericyte adhesion and endothelial basement membrane formation during angiogenesis. *PLoS One* **7,** e30562 CrossRef Medline

40. Crawford, L. A., Guney, M. A., Oh, Y. A., Deyoung, R. A., Valenzuela, D. M., Murphy, A. J., Yancopoulos, G. D., Lyons, K. M., Brigstock, D. R., Economides, A., and Gannon, M. (2009) Connective tissue growth factor (CTGF) inactivation leads to defects in islet cell lineage allocation and β-cell proliferation during embryogenesis. *Mol. Endocrinol.* **23,** 324–336 CrossRef Medline

41. Chng, S. C., Ho, L., Tian, J., and Reversade, B. (2013) ELABELA: A hormone essential for heart development signals via the apelin receptor. *Dev. Cell* **27,** 672–680 CrossRef Medline

42. Pauli, A., Norris, M. L., Valen, E., Chew, G. L., Gagnon, J. A., Zimmerman, S., Mitchell, A., Ma, J., Dubrulle, J., Reyon, D., Tsai, S. Q., Joung, J. K., Saghatelian, A., and Schier, A. F. (2014) Toddler: An embryonic signal that promotes cell movement via Apelin receptors. *Science* **343,** 1248636 CrossRef Medline

43. Kanazawa, K., Azuma, Y., Nakano, H., and Kudo, A. (2003) TRAF5 functions in both RANKL- and TNFα-induced osteoclastogenesis. *J. Bone Miner. Res.* **18,** 443–450 CrossRef Medline

44. Emery, B., and Dugas, J. C. (2013) Purification of oligodendrocyte lineage cells from mouse cortices by immunopanning. *Cold Spring Harb. Protoc.* **2013,** 854–868 CrossRef Medline

45. Okuda, S., Watanabe, Y., Moriya, Y., Kawano, S., Yamamoto, T., Matsumoto, M., Takami, T., Kobayashi, D., Araki, N., Yoshizawa, A. C., Tabata, T., Sugiyama, N., Goto, S., and Ishihama, Y. (2017) jPOSTrepo: An international standard data repository for proteomes. *Nucleic Acids Res.* **45,** D1107–D1111 CrossRef Medline

46. Kitagawa, M., Hatakeyama, S., Shirane, M., Matsumoto, M., Ishida, N., Hattori, K., Nakamichi, I., Kikuchi, A., Nakayama, K., and Nakayama, K. (1999) An F-box protein, FWD1, mediates ubiquitin-dependent proteolysis of β-catenin. *EMBO J.* **18,** 2401–2410 CrossRef Medline

47. Kamura, T., Hara, T., Kotoshiba, S., Yada, M., Ishida, N., Imaki, H., Hatakeyama, S., Nakayama, K., and Nakayama, K. I. (2003) Degradation of p57[Kip2] mediated by SCF[Skp2]-dependent ubiquitylation. *Proc. Natl. Acad. Sci. U.S.A.* **100,** 10231–10236 CrossRef Medline

48. Hirano, A., Yumimoto, K., Tsunematsu, R., Matsumoto, M., Oyama, M., Kozuka-Hata, H., Nakagawa, T., Lanjakornsiripan, D., Nakayama, K. I., and Fukada, Y. (2013) FBXL21 regulates oscillation of the circadian clock through ubiquitination and stabilization of cryptochromes. *Cell* **152,** 1106–1118 CrossRef Medline

ASBMB

J. Biol. Chem. (2018) 293(15) 5705–5714 **5713**

49. Kamura, T., Sato, S., Iwai, K., Czyzyk-Krzeska, M., Conaway, R. C., and Conaway, J. W. (2000) Activation of HIF1α ubiquitination by a reconstituted von Hippel-Lindau (VHL) tumor suppressor complex. *Proc. Natl. Acad. Sci. U.S.A.* **97,** 10430 –10435 CrossRef Medline

50. Kamura, T., Hara, T., Matsumoto, M., Ishida, N., Okumura, F., Hatakeyama, S., Yoshida, M., Nakayama, K., and Nakayama, K. I. (2004) Cytoplasmic ubiquitin ligase KPC regulates proteolysis of p27^{Kip1} at G$_1$ phase. *Nat. Cell Biol.* **6,** 1229 –1235 CrossRef Medline

51. Katayama, Y., Nishiyama, M., Shoji, H., Ohkawa, Y., Kawamura, A., Sato, T., Suyama, M., Takumi, T., Miyakawa, T., and Nakayama, K. I. (2016) CHD8 haploinsufficiency results in autistic-like phenotypes in mice. *Nature* **537,** 675– 679 CrossRef Medline